

## Redox Transitions in an Electrolyte-Free Myoglobin Fluid

Kamendra P. Sharma,<sup>†</sup> Kieren Bradley,<sup>†</sup> Alex P. S. Brogan,<sup>†</sup> Stephen Mann,<sup>\*,†</sup> Adam W. Perriman,<sup>\*,†,‡</sup> and David J. Fermin<sup>\*,†</sup>

<sup>†</sup>School of Chemistry, Cantocks Close, University of Bristol, BS8 1TS, United Kingdom

<sup>‡</sup>School of Cellular and Molecular Medicine, University of Bristol, BS8 1TD, United Kingdom

### S Supporting Information

**ABSTRACT:** Redox responses associated with the heme prosthetic group in a myoglobin-polymer surfactant solvent-free liquid are investigated for the first time in the absence of an electrolyte solution. Cyclic voltammograms from the biofluid exhibit responses that are consistent with planar diffusion of mobile charges in the melt. Temperature-dependent dynamic electrochemical and rheological responses are rationalized in terms of the effective electron hopping rate between heme centers and the transport of intrinsic ionic species in the viscous protein liquid.

Core biological processes such as respiration, photosynthesis, and metabolism are fundamentally dependent on ensembles of redox enzymes that regulate electron flow and chemical reactivity.<sup>1,2</sup> The conceptual framework that describes these complex and highly tuned reactions has been exploited for the fabrication of numerous devices ranging from bioreactors to biosensors.<sup>3–6</sup> In practice, this involves the integration of redox-active proteins into hybrid electrocatalytic cells that can be regulated by the application of an external bias without the need for large electrode overpotentials. Moreover, enzyme electrocatalysts offer high levels of chemical specificity, although significant challenges associated with the effective integration of proteins into functional devices still remain.

Myoglobin is a redox-active globular protein that regulates dioxygen levels in myocytes and has been the focus of many electrochemical studies due to its natural abundance and well-characterized structure. The redox activity of myoglobin arises from its heme prosthetic group that is moderated by the surrounding structure of the globular fold, which promotes high levels of oxygen affinity in the ferrous state.<sup>7</sup> Conversely, in the ferric state, myoglobin has a five coordinate geometry where the sixth coordination site is occupied by a loosely bound water molecule (met-myoglobin).<sup>7</sup> Accordingly, induced redox transformations of ferrous deoxymyoglobin often need to be performed under an inert atmosphere to inhibit oxygen binding. Moreover, the use of aqueous formulations of native myoglobin to carry out heterogeneous electron transfer reactions at electrode surfaces has been shown to be problematic due to a number of intrinsic factors including adsorption-induced protein denaturation, inaccessibility of the prosthetic redox center due to obstruction by the polypeptide chain, and the lack of orientational compatibility between the protein and electrode.<sup>6</sup> Consequently, a variety of approaches

have been used in an effort to overcome these limitations, including the fabrication of solid hybrid myoglobin-polymer electrode coatings using layer-by-layer (LBL) assembly. For example, polysaccharides (hydroxyethyl cellulose ethoxylate and hyaluronic acid),<sup>8</sup> DNA,<sup>9</sup> poly(diallyl dimethyl) ammonium chloride (PDDA),<sup>9</sup> and poly(styrenesulphonate) (PSS)<sup>9,10</sup> have been used as alternating layers in myoglobin LBL film preparations. Redox active thin film electrode coatings containing Fe(II)/Fe(III) coupled heme proteins have also been produced using sodium dodecylsulphate (SDS), dimyristoylphosphatidylcholine (DMPC), or didodecyldimethylammonium bromide (DDAB).<sup>11,12</sup> In the past, a few studies have also focused on encapsulating myoglobin in hydrated polyelectrolytes,<sup>13</sup> and although these approaches have been applied to successfully retain protein activity and stability, performance remains acutely dependent on the aqueous environment.

Here we report on an entirely new approach in which the redox activity of myoglobin is directly addressed in a highly crowded anhydrous biomolecular myoglobin-polymer surfactant liquid (hereafter referred to as a myoglobin melt) in the absence of deliberately added electrolyte solution. The directed electrostatic coupling of polymer surfactant chains to the protein surface provides access to not only an anhydrous liquid phase but also a self-contained soft electrolytic medium between the redox centers of the myoglobin molecules. The novel biofluid construct described herein offers a wide portfolio of benefits for bioelectrochemistry, including an exceptionally high concentration of protein molecules ( $\approx 270 \text{ mg cm}^{-3}$ ) with remarkable levels of thermal stability (half denaturation temperature of  $160 \text{ }^\circ\text{C}$ ),<sup>14</sup> persistent protein dynamics,<sup>15</sup> and sustained biological function.<sup>16</sup> Dynamic electrochemical data suggest the development of planar diffusion profiles, which are interpreted in terms of electron hopping between adjacent heme prosthetic groups. These findings have significant implications on the design of bioinspired electrocatalysts for sensing and energy applications.

Met-myoglobin melts were produced using methodology which has been described previously (see Supporting Information, Methods).<sup>15</sup> Briefly, this involved protein cationization *via* *N*-(3-dimethylaminopropyl)-*N'*-ethylcarbodiimide (EDC)-mediated coupling of 3-(dimethylamino)-1-propylamine (DMAPA) to the protein surface, followed by electrostatic addition of the anionic polymer surfactant 4-

Received: October 11, 2013

Published: November 18, 2013

nonylphenyl-3-sulfopropyl ether ( $S_1$ ) to the cationized protein to yield a cationized myoglobin-polymer surfactant conjugate ( $S_1$ -cMb) with a protein charge to polymer surfactant ratio of ca. 1:1 (Figure 1a). Dynamic light scattering from the aqueous

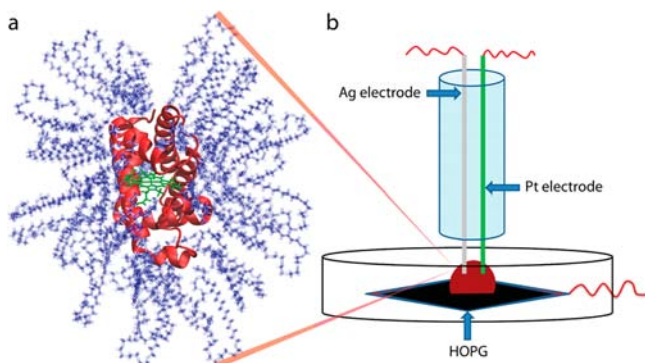


**Figure 1.** (a) Molecular model of the cationized myoglobin-polymer surfactant conjugate ( $S_1$ -cMb) formed by coupling 3-(dimethylamino)-1-propylamine (DMAPA) to the acidic side chains of myoglobin, followed by electrostatic addition of 4-nonylphenyl-3-sulfopropyl ether ( $S_1$ ). (b) Schematic diagram showing the three electrode cell configuration, where Pt (counter) and Ag (pseudoreference) wires are inserted directly into a drop of the  $S_1$ -cMb melt, which is in contact with a highly oriented pyrolytic graphite (HOPG) electrode.

$S_1$ -cMb conjugate gave a hydrodynamic diameter of 3.8 ( $\sigma \approx 1.2$ ) nm, which was consistent with a protein enclosed by a high-density sheath of polymer surfactant molecules (Supporting Information, Figure S1). The aqueous hybrid construct ( $S_1$ -cMb) was subsequently lyophilized for 48 h and annealed at 40 °C, yielding a viscous room-temperature fluid with an effective protein concentration of approximately 270 mg mL<sup>-1</sup>. Differential Scanning Calorimetry (DSC) from the  $S_1$ -cMb melt showed a single endothermic melting transition peak at 22–23 °C (Supporting Information, Figure S2), and diffuse reflectance UV–vis (DR-UV–vis) spectroscopy gave a Soret band peak maximum of 414 nm, which was consistent with a low-spin met-Mb heme metallocenter (Supporting Information, Figure S3).<sup>16</sup> Electrochemical data were recorded (see Supporting Information, Methods) using a three-electrode configuration, in which Pt (counter) and Ag (pseudoreference) wires were inserted directly into a ca. 50 mg drop of the  $S_1$ -cMb melt, which was deposited onto a highly oriented pyrolytic graphite (HOPG) electrode (Figure 1b). The cell was kept under a positive pressure of Ar gas, and the temperature was regulated using a Linkam thermal stage.

The key feature present in all cyclic voltammetric responses recorded at 25 °C was the quasi-reversible one-electrode response centered at approximately –0.23 V (Figure 2). Since all of the materials employed in the preparation of the myoglobin melt are electrochemically inert, this signal can be unambiguously assigned to the changes in the oxidation state of the heme moiety. Moreover, the responses resemble the characteristic electrochemical signature observed for myoglobin assemblies in aqueous electrolyte.<sup>2</sup>

The voltammograms recorded at 25 °C (Figure 2a) exhibit a number of interesting features associated with the peak-to-peak potential difference ( $\Delta E_{\text{peak}}$ ), the anodic to cathodic peak current ratio ( $i_{\text{c,peak}}/i_{\text{a,peak}}$ ), and the cathodic peak current scan rate ( $\nu$ ) dependence.  $\Delta E_{\text{peak}}$  increased marginally with increasing scan rate from 112 mV at 10 mV s<sup>-1</sup> to 128 mV

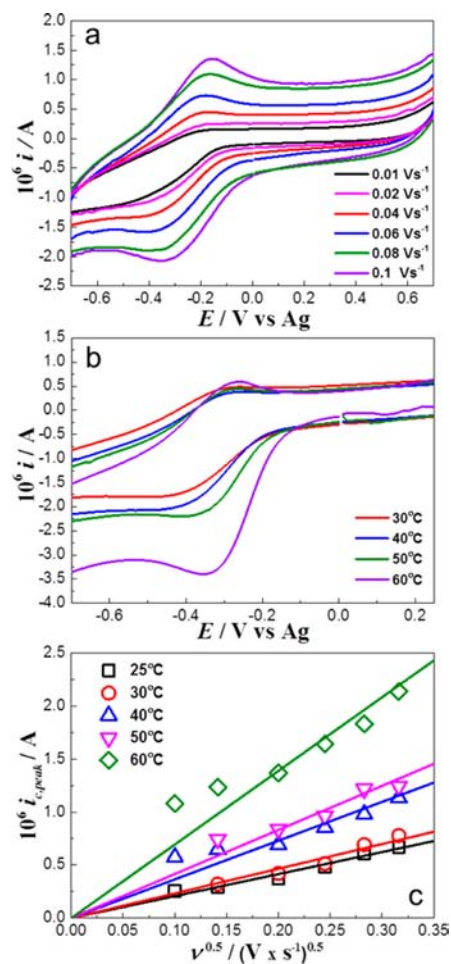


**Figure 2.** (a) Cyclic voltammograms of the  $S_1$ -cMb melt at 25 °C and scan rates ( $\nu$ ) ranging from 0.01 to 0.10 V s<sup>-1</sup>. (b) Cyclic voltammograms of  $S_1$ -cMb at various temperatures at 0.10 V s<sup>-1</sup>. (c) Cathodic peak current ( $i_{\text{c,peak}}$ ) as a function of  $\nu^{0.5}$  at different temperatures. Experiments were recorded using a HOPG electrode (0.25 cm<sup>2</sup>) and Ag wire acting as a quasi-reference electrode.

at 100 mV s<sup>-1</sup>, while the  $i_{\text{a,peak}}/i_{\text{c,peak}}$  ratio also increased from ca. 0.24 to 0.94 over this range. Both trends are consistent with complex charge transport dynamics in the protein melt, with a coupled chemical reaction involving the reduced state of the heme. In aqueous electrolyte solutions in the presence of oxygen, the reduced heme readily catalyzes the formation of H<sub>2</sub>O<sub>2</sub>.<sup>10</sup> However, thermogravimetric analysis of  $S_1$ -cMb (Supporting Information, Figure S4) shows that water content is below 0.35% w/w, which is in agreement with previous studies on similar melts.<sup>16</sup> This equates to approximately 11–12 water molecules per protein, which is far below the several hundred water molecules needed to form a full hydration shell around small globular proteins such as myoglobin. Although it is clear that O<sub>2</sub> is playing a role in the coupled chemical reaction with the reduced heme, the mechanism involved in such an anhydrous environment remains to be elucidated. It should also be mentioned that small quantities of O<sub>2</sub> are expected in the melt even under an Ar atmosphere, considering the high viscosity of the biofluid at room temperature. This is consistent with the equilibrium oxygen diffusion experiments performed on a solvent-free myoglobin liquid, which showed that the oxygen binding process was limited by Stokes–Einstein diffusion, occurring on a scale of several minutes.<sup>16</sup> Moreover,

the time scale of the electrochemical experiments were several orders of magnitude longer than any typical changes in protein conformation.<sup>17</sup>

The temperature dependence of the voltammetric responses at  $\nu = 100 \text{ mV s}^{-1}$  (Figure 2b) provided further information on the nature of the interfacial electrochemical process, *i.e.*, a systematic increase in the  $i_{c,\text{peak}}$  was observed with increasing temperature, while the changes in  $i_{a,\text{peak}}$  were less significant. A small decrease in  $\Delta E_{\text{peak}}$  was also observed with increasing temperature (see also cyclic voltammograms at various scan rates and temperatures in the Supporting Information, Figures S5 to S8). These observations are indicative of an increase in the electron transfer rate at the melt/HOPG interface. Furthermore, the increase in  $i_{c,\text{peak}}$  suggested an increase in the effective diffusion coefficient of transport limiting species. This behavior is clearly illustrated by the dependence of  $i_{c,\text{peak}}$  on the square root of the scan rate (Figure 2c), suggesting that the kinetics of the electrochemical responses were controlled by planar diffusion to the electrode surface. It should be mentioned that the coupled chemical reaction affects the intensity and position of cathodic peak current, in particular at low scan rates. Other issues such as the kinetics of electron transfer should also be considered when analyzing the scan rate dependence of  $i_{c,\text{peak}}$ . However, for the sake of simplicity, it is assumed that the electrochemical responses are mainly controlled by diffusion.

Dynamic viscosity ( $\eta$ ) was estimated from rheology measurements (Supporting Information, Figure S9) as a function of temperature (Figure 3a), and the data clearly show a sharp decrease of  $\eta$  with temperature in the range of 20 to 30 °C. The integrity of the protein secondary structure in the melt is retained in this temperature range, as indicated by synchrotron radiation circular dichroism measurements carried out on similar myoglobin melts, which showed a decrease in the  $\alpha$ -helical content of only 3% between 25 and 60 °C.<sup>14</sup> Furthermore, diffuse reflectance UV–vis spectroscopy measurements performed on the myoglobin melt showed only a minimal blue shift and a 4.7% decrease in the intensity of the Soret band between 25 and 60 °C (Supporting Information, Figure S3), confirming that no major changes in the protein tertiary structure in the vicinity of the heme moiety occurred over this temperature range.

The temperature dependence of the effective diffusion coefficient ( $D_{\text{CV}}$ ) (Figure 3b) was estimated from the voltammetric data using a protein concentration in the melt of  $15.8 \times 10^{-6} \text{ mol cm}^{-3}$ .<sup>18</sup> The results show an increase in  $D_{\text{CV}}$  from approximately  $0.4$  to  $5.0 \times 10^{-11} \text{ cm}^2 \text{ s}^{-1}$  over the temperature range investigated. These values are several orders of magnitude lower than those reported in myoglobin-DDAB surfactant films assembled at the electrode/aqueous electrolyte interface.<sup>11</sup> The  $D_{\text{CV}}$  values obtained from the electrochemical analysis are compared with those estimated by applying the Stokes–Einstein relationship ( $D_{\text{SE}}$ ) to the hydrodynamic viscosity data shown in Figure 2a, where the myoglobin center–to–center distance (5.30 nm) was estimated from small-angle X-ray scattering experiments performed on the myoglobin melt (Supporting Information, Figure S10). Significantly, it can be seen that  $D_{\text{CV}}$  is approximately 1 order of magnitude larger than  $D_{\text{SE}}$ , suggesting that the electrochemical responses were not controlled by the diffusion of the whole myoglobin construct.

Changes in the heme oxidation state are generally accompanied by a charge compensation step involving mobile

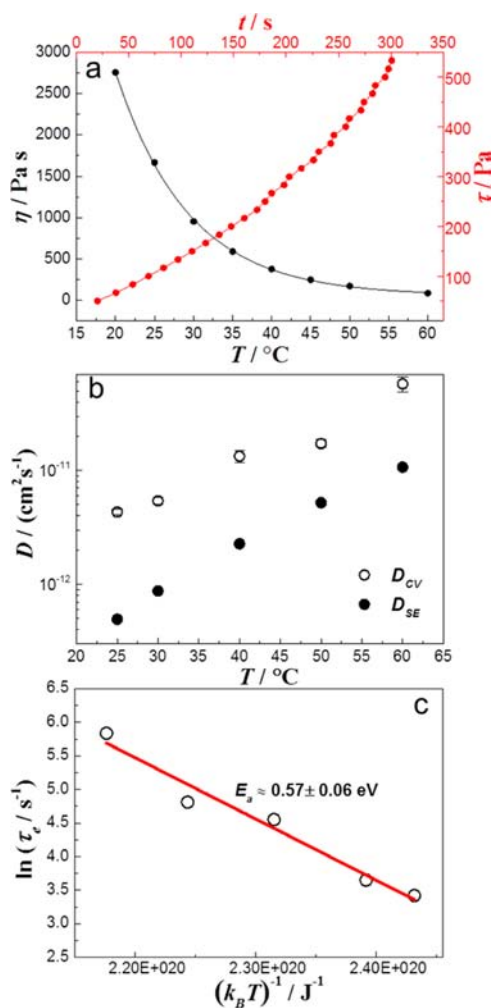


**Figure 3.** (a) Hydrodynamic viscosity ( $\eta$ ) as a function of temperature and time dependence of the shear stress ( $\tau$ ) of S<sub>1</sub>-cMb. (b) Effective diffusion coefficients ( $D_{\text{CV}}$ ) estimated from the voltammetric analysis in Figure 2c and the Stokes–Einstein equation ( $D_{\text{SE}}$ ) assuming the diffusion of S<sub>1</sub>-cMb conjugate. (c) Hopping frequency ( $\tau_c$ ) in the myoglobin melt as a function of temperature, calculated using the apparent diffusion coefficient and heme-to-heme distance.

ionic species. Although the methodology for the preparation of S<sub>1</sub>-cMb involves extensive dialysis steps, the presence of small ionic species as a result of charge overcompensation during protein cationization and polymer surfactant addition cannot be entirely excluded. Consequently, a hopping mechanism in which electrons diffuse from heme-to-heme moieties coupled with the transport of a mobile ionic species is possible. Taking the heme-to-heme distance as  $2r$ , the hopping frequency ( $\tau_c$ ) was evaluated as a function of temperature (Figure 3c),<sup>19</sup> and linear regression yielded a hopping activation energy ( $E_a$ ) of  $0.57 \pm 0.06 \text{ eV}$ . These values are comparable with charge transport in conjugated molecular wires ranging in length from 3.1 to 9.4 nm.<sup>20</sup>

Based on our observations, the most likely charge transport mechanism in these highly viscous protein melts can be rationalized as *polaron type* structures, *i.e.*, electron hopping from heme-to-heme centers coupled with intrinsic mobile ionic species. These processes can be described in terms of the electron self-exchange rate constant ( $k_{\text{EX}}$ ) as defined by the Dahms–Ruff model.<sup>21,22</sup> Murray and co-workers have studied the electron and mass transport in melts of polyether-tailed

metalloporphyrins and found that the electron hopping is approximately 2 orders of magnitude higher than ionic diffusion.<sup>23,24</sup> It could be estimated that  $k_{\text{EX}}$  in the S<sub>1</sub>-cMb melt increases from  $5.8 \times 10^3$  to  $6.5 \times 10^7 \text{ M}^{-1} \text{ s}^{-1}$  upon increasing the temperature from 25 to 60 °C.<sup>25</sup> These values are 3 orders of magnitude lower than those reported for the polyether-metalloporphyrin complex melts, which are characterized by a 1–2 nm center-to-center distance. As mentioned above, this distance in the S<sub>1</sub>-cMb melt is significantly larger (5.3 nm), which is consistent with the slower transport rate.

To summarize, we demonstrate for the first time that the redox properties of myoglobin can be electrochemically addressed in a solvent-free myoglobin melt at temperatures as high as 60 °C. Cyclic voltammograms are characterized by a quasi-reversible one-electron transfer step with planar diffusion profiles. Analysis of the electrochemical data, based on structural information of the protein conjugate obtained from diffuse reflectance UV–vis, SAXS, and rheology measurements, suggests that charge transport occurs *via* electron hopping from heme-to-heme coupled with the migration of mobile ionic species. These studies open a new area in the field of bioelectrocatalysis, in which the active components can be stored as a high density fluid at an electrode surface where the biological scaffold is protected by the polymer surfactant corona. Indeed, previous studies show that these solvent-free protein liquids can be refolded from 155 °C with ~95% efficiency.<sup>14</sup> Furthermore, we believe this approach could provide a new generation of biologically inspired charge transporting media, with tunable conductivities and chemical functionalities, which could be exploited in a wide range of sensing applications.

## ■ ASSOCIATED CONTENT

### ■ Supporting Information

Methods and experimental, dynamic light scattering, differential scanning calorimetry, diffuse reflectance (UV–vis), thermogravimetric analysis, cyclic voltammograms at various temperatures, rheology, and small-angle X-ray scattering of S<sub>1</sub>-cMb melt. This material is available free of charge via the Internet at <http://pubs.acs.org>.

## ■ AUTHOR INFORMATION

### ■ Corresponding Authors

S.Mann@bristol.ac.uk (S.M.)  
chawp@bristol.ac.uk (A.W.P.)  
David.fermin@bristol.ac.uk (D.J.F.)

### ■ Notes

The authors declare no competing financial interest.

## ■ ACKNOWLEDGMENTS

We gratefully acknowledge fruitful discussions with Dr. Ross Anderson and Dr. Daniela Plana, Prof. Robert Richardson for access to his SAXS facility, Dr. John Chew and Dr. Valeska Ting for assistance with rheometry, Dr. Richard Sessions for the model in Figure 1, and the EPSRC (Cross-disciplinary interfaces program), Leverhulme Trust (RPG-2013-103), and ERC (Advanced Grant) for financial support.

## ■ REFERENCES

- (1) Moser, C.; Page, C.; Farid, R.; Dutton, P. L. *J. Bioenerg. Biomembr.* **1995**, *27*, 263.
- (2) Gray, H. B.; Winkler, J. R. *Annu. Rev. Biochem.* **1996**, *65*, 537.
- (3) Liu, C.-Y.; Hu, J.-M. *Biosens. Bioelectron.* **2009**, *24*, 2149.

(4) Hu, S.; Lu, Q.; Xu, Y. *Electrochemical Sensors, Biosensors and their Biomedical Applications*; Academic Press: San Diego, 2008; p 531.

(5) Arya, S. K.; Solanki, P. R.; Datta, M.; Malhotra, B. D. *Biosens. Bioelectron.* **2009**, *24*, 2810.

(6) Rusling, J. F. *Acc. Chem. Res.* **1998**, *31*, 363.

(7) Pauling, L. *Nature* **1964**, *203*, 182.

(8) Liu, Y.; Liu, H.; Guo, X.; Hu, N. *Electroanalysis* **2010**, *22*, 2261.

(9) Lvov, Y. M.; Lu, Z.; Schenkman, J. B.; Zu, X.; Rusling, J. F. *J. Am. Chem. Soc.* **1998**, *120*, 4073.

(10) Ma, H.; Hu, N.; Rusling, J. F. *Langmuir* **2000**, *16*, 4969.

(11) Rusling, J. F.; Nassar, A.-E. F. *J. Am. Chem. Soc.* **1993**, *115*, 11891.

(12) Zhang, Z.; Nassar, A.-E. F.; Lu, Z.; Schenkman, J. B.; Rusling, J. F. *J. Chem. Soc., Faraday Trans.* **1997**, *93*, 1769.

(13) Ohno, H. *J. Macromol. Sci., Part A* **1994**, *31*, 83.

(14) Brogan, A. P. S.; Siligardi, G.; Hussain, R.; Perriman, A. W.; Mann, S. *Chem. Sci.* **2012**, *3*, 1839.

(15) Gallat, F.-X.; Brogan, A. P. S.; Fichou, Y.; McGrath, N.; Moulin, M.; Härtlein, M.; Combet, J.; Wuttke, J.; Mann, S.; Zaccai, G.; Jackson, C. J.; Perriman, A. W.; Weik, M. *J. Am. Chem. Soc.* **2012**, *134*, 13168.

(16) Perriman, A. W.; Brogan, A. P. S.; Cölfen, H.; Tsoureas, N.; Owen, G. R.; Mann, S. *Nat. Chem.* **2010**, *2*, 622.

(17) Lim, M.; Jackson, T. A.; Anfinrud, P. A. *Proc. Natl. Acad. Sci. U.S.A.* **1993**, *90*, 5801.

(18) Effective diffusion coefficient ( $D_{\text{CV}}$ ) was estimated from the Randles–Sevcik expression,

$$i_{\text{c,peak}} = 0.4463nFAc_m \left( \frac{nFvD_{\text{CV}}}{RT} \right)^{1/2}$$

where  $n$ ,  $F$ ,  $A$ ,  $T$ ,  $c_m$ , and  $v$  are the number of electrons transferred, Faraday's constant, the electrode surface area ( $0.25 \text{ cm}^2$ ), temperature, concentration of myoglobin in the melt ( $15.8 \times 10^{-6} \text{ mol cm}^{-3}$ ), and the scan rate in  $\text{V s}^{-1}$ .

(19) The electron hopping frequency ( $\tau_e$ ) was estimated using  $D_{\text{CV}}$ :  $\tau_e = 2D_{\text{CV}}/(2r)^2$ , where  $r$  is the effective radius of the conjugate.

(20) Hines, T.; Diez-Perez, I.; Hihath, J.; Liu, H.; Wang, Z.-S.; Zhao, J.; Zhou, G.; Müllen, K.; Tao, N. *J. Am. Chem. Soc.* **2010**, *132*, 11658.

(21) Dahms, H. *J. Phys. Chem.* **1968**, *72*, 362–364.

(22) Ruff, I.; Friedrich, V. *J. Phys. Chem.* **1971**, *75*, 3297–3302.

(23) Long, J. W.; Kim, I. K.; Murray, R. W. *J. Am. Chem. Soc.* **1997**, *119*, 11510–11515.

(24) Lee, D.; Hutchison, J. C.; Leone, A. M.; DeSimone, J. M.; Murray, R. W. *J. Am. Chem. Soc.* **2002**, *124*, 9310–9317.

(25) The electron self-exchange rate constants ( $k_{\text{EX}}$ ) at different temperatures were estimated using the relation:  $k_{\text{EX}} = 3\tau_e/c_m$ .